Dušan Čurćija, Ilija Mamuzić

ESTIMATION OF LUBRICANT LAYER ON PIPE ROLLING IN MILLS

Abstract

Approximate analysis of lubricant layer at seamless pipe conti-rolling in working mills. The thickness of lubricant laye is in micros and nanos, and it is expressed through the lubrication equation (Reynold's differential equation). The solution is deduced for smooth surfaces of tools and pipes regardless of the inertial forces of lubricants at higher operating rate. Lubricant ecological characteristics and tool geometrical characteristics were analysed. Analytical solutions were tested in several mathematical programmes and compared to Monte-Carlo method within the program Mathematica.

Introduction

Pipe rolling in circular calibers [1] is a form of transversal rolling where the deformation zone usually includes a pair of operating rolls and a mandrel (Figure 1). Pipe rolling on a long floating mandrel is used on a continous rolling mill with 7 to 9 stands. Before placing a tube between the rolls, a long cylindrical mandrel is inserted in which than moves with the tube in the deformation zone. The rate of the mandrel is lower than the rate of the front of the pipe at the exit from the rolls, but it is faster than the rate of the end of the pipe at the entrance into the rolls. The features of speed conditions in caliber rolling influence the rate of pipes and rolls in each section of the deformation zone and are equal only at two points of the caliber.

In this way, the curve of equal rate of pipes and rolls demarcates the zones of relative metal slide on the surface – the advance zone and the lag zone. Experiments proved that with pipe rolling in calibers there is an advance zone at the top of a caliber, and, as a rule, there is a lag zone in the roll gap (Figure 2).

The pipe rolling processes on continous mills have been developed using a long immobile cylindrical, conical or gradient mandrel. This kind of rolling is special due to two subzones in the deformation zone: a diameter reduction zone and a pipe wall reduction zone according to Fig. 1. The external contact [2,3] of pipes and rolls without addition of lubricant, is governed by Kulon-Amonton's laws of friction, while

between the mandrel and the inner surface of the tube, due to the lubricant, is governed by Newton's fluid friction laws.
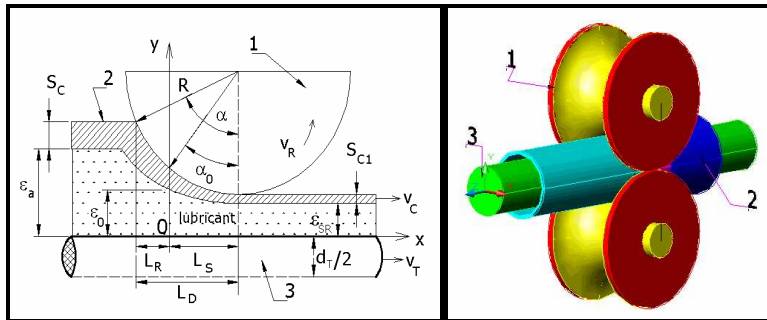

Figure 1: Rolling scheme of seamless pipe (2) between rolls (1) and with the mandrel (3)

The values of tangential stress in the lubricant film [4,5] is described with the differential equation (1):

$$\tau_x = \mu^*(v_C - v_T)\frac{1}{\varepsilon(x)} - \frac{1}{2}\varepsilon(x)*\frac{\partial p}{\partial x}$$

(1)

The change of pressure gradient in the lubricant layer [4,5,6,7] is described with the differential equation (2) and the volume of consumption of lubricant over the pipe perimeter [6,7] is described with the expression (3).

$$\frac{dp}{dx} = \frac{6\mu(v_C + v_T)}{\varepsilon^2(x)} - \frac{12\mu Q}{\varepsilon^3(x)}$$

(2)

$$Q(x) = \int\limits_{0}^{\varepsilon(x)} u\,dy = -\frac{1}{12\mu}\frac{dp}{dx}\varepsilon^3(x) + \left(\frac{v_C + v_T}{2}\right)\varepsilon(x)$$

(3)

The geometry of lubricant contact [8,9,10] and the length of lubricating wedge are described with the expression (4) and (5)

$$\varepsilon(x) = \varepsilon_0 + R_0\left[\cos\alpha_0 - \sqrt{1 - \left(\sin\alpha_0 - \frac{x}{R_0}\right)^2}\right]$$

(4)

$$a = R_0\left[\sqrt{1 - \left(\cos\alpha_0 - \frac{\varepsilon_a}{R_0} + \frac{\varepsilon_0}{R_0}\right)^2} - \sin\alpha_0\right]$$

(5)

$$\varepsilon(x) = \varepsilon_0 - \alpha_0 x + \frac{x^2}{2R_0} - \frac{\alpha_0 x^3}{2R_0{}^2} + \frac{x^4}{8R_0{}^3}$$
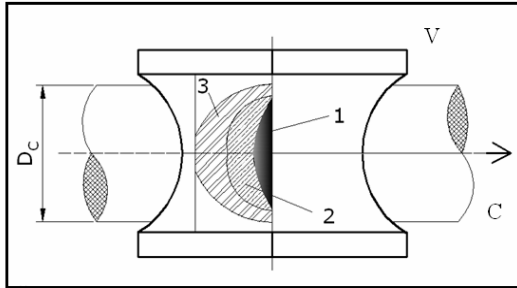
(6)

Figure 2: Distribution of zones of relative slide in circular calibers: 1-a small advance zone, 2-a medium neutral cut zone, 3-an advance along the total length of the deformation zone at the top of a caliber

The expression (6) is the developpment [11,12,13] of the equation (4) in Maclaurin's series. The lubricant properties for theoretical research and process geometry are taken from the relevant references of Russian and Ukrainian authors and are given in Table 1.

Table 1: Typical lubricant properties for theoretical estimation

Parameter	Value	Unit
γ-piezo coefficient of viscosity	2,18E-7	Pa^{-1}
p_0-rolls pressure	20E6	Pa
V_C-motion speed of tube blank	8,5	m/s
V_T-mandrel speed	7,5	m/s
R-roll radius	0,197 (0.50)	m
S_{C2}	0,003 (0.0271)	m
μ_0-dinamic viscosity of lubricant $\mu = \mu_0 \exp(\gamma^* p_0)$	0,024-0.048	Pas
α_0-angle of engagement	0-0,02	rad
ε_a-height of mandrel lubricant	1,0E-3-1,0E-7	m
A-technological parameter	1,965512E6	m^{-1}
$A = [1 - \exp(-\gamma^* p_0) / 6\mu_0 \gamma (v_C + v_T)]$		
Smooth surfaces of tube blanks and mandrel are supposed $R_0 = R + S_{C2}$		

2. Solutions of differential equations

Approximate analytical solutions of equation (2) are shown in Table 2. All numerical estimations were obtained using the mathematical programme MathCad Professional in accordance to the different zones in Figure 3.
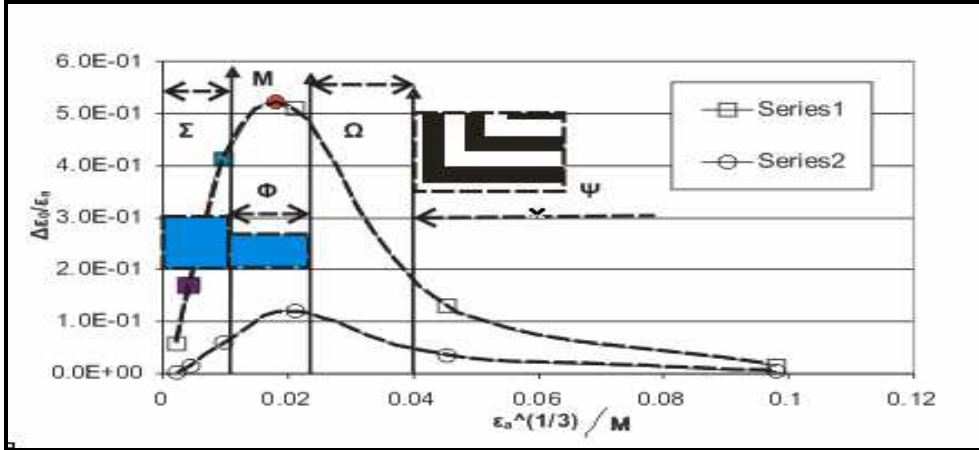

Figure 3: Systematization of analytical solutions in Table 2 shown through the relative lubricant layer thickness. The point M in the maximum of the graphic scheme determines the numerical method Monte-Carlo.

Series 1- $\left(\varepsilon_0^1 - \varepsilon_0^{0.1}\right)/\varepsilon_a$; $\varepsilon_0^{0.1}$ - lubricant height for the engagement angle 0,1 rad

Series 2- $(\varepsilon_0^1 - \varepsilon_0^*)/\varepsilon_a$

In table 3 the comparison of the Monte-Carlo method appčlied within the mathematical program and the analytical solutions according to Table 2 are shown. Some solutions from the Table 3 are determines applying the Solver in the mathematical program MATLAB and the Excel's Solver for D=0 of the expression (6) when the approximate analytical solutions are obtained through square trinomials. In these programs some multi complex analytical solutions (which are not suitable for fast practical estimation) were controlled and compared to the mathematical method Monte-Carlo. Afterwards, they were simplified and presented in the Table 2.

The sufficient accuracy of the solution in the point M determines the numerical method Monte-Carlo. In the zones Φ and Σ the solutions become closer with more intensive "lubricant milling" in mills that can be deduced applying the equation (7).

Table 2: Approximate analytical solution of equation (2) according to Figure 3.

Zone of Fig.3	Approximate analytical solution
Ψ	$\varepsilon_0^* = 0.7726\varepsilon_0^1 \qquad \varepsilon_0^* = 0.5R_0(\alpha^*)^2 \qquad \alpha^* = \sqrt[3]{\dfrac{8}{15R_0A}}$
Ω	$\alpha^* = 2*\sqrt[3]{\dfrac{\varepsilon_a\sqrt{2R_0\varepsilon_a}}{10R_0{}^2 + 15R_0A\varepsilon_a\sqrt{2R_0\varepsilon_a}}} \qquad \varepsilon_0^* = \dfrac{R_0(\alpha^*)^2}{2}$
M	$\alpha_0^* = \left(\dfrac{2}{5}\right)^2 \dfrac{1}{A\varepsilon_{aMAX}} \qquad \varepsilon_0^* = \dfrac{R_0(\alpha_0^*)^2}{2} \qquad \varepsilon_{aMAX} = 0.28674*\sqrt[3]{\dfrac{R_0}{A^2}}$
Φ Σ	$\varepsilon_0^1 = \varepsilon_a\left(1 - \dfrac{0.57348*\varepsilon_a}{\varepsilon_{aMAX}}\right) \qquad \varepsilon_{aMAX} = 0.28674*\sqrt[3]{\dfrac{R_0}{A^2}}$
Note: indices (0 and *) refer to discriminant of the trinomial on the second power in the expression (6) that aspires to zero. Indices (0 and 1) are given for the case when $\alpha_0 \rightarrow 0$ rad. ε_{aMAX}=height of lubricant layer on the mandrel at which a maximum of Figure 3 is achieved is shown in Table 1. $R_0=R+S_{C2}$	

Table 3: Comparison of the Monte-Carlo numerical method and analytical solution of equation according to the Table 2 and the Figure 3

ε_a /m	Monte-Carlo ε_0^* /m	Zone Ω ε_0^* /m	Point M ε_0^* /m	Zone Φ i Σ ε_0^1 /m
9.420E-04	1.225E-05	1.225E-05	-	-
8.735E-05	1.136E-05	1.129E-05	-	-
1.069E-05	**5.801E-06**	-	**5.801E-06**	-
7.425E-06	4.618E-06	-	-	4.466E-06
6.849E-06	4.373E-06	-	-	4.332E-06
1.210E-06	1.065E-06	-	-	1.081E-06
2.456E-07	2.362E-07	-	-	2.404E-07
1.205E-07	1.178E-07	-	-	1.192E-07
3.846E-08	3.809E-08	-	-	3.833E-08
1.046E-08	1.042E-08	-	-	1.045E-08
7.986E-09	7.962E-09	-	-	7.981E-09
4.123E-09	4.115E-09	-	-	4.121E-09
9.682E-09	9.676E-09	-	-	9.676E-09
3.141801E-10	3.1409E-10	-	-	3.1417E-10
3.141590E-11	K=K(ε_0)			

$$\varepsilon_0^l = \varepsilon_a \left(1 - \frac{0.57348 * \varepsilon_a}{\varepsilon_{aMAX}} \right) \qquad \varepsilon_{aMAX} = 0.28674 * \sqrt[3]{\frac{R_0}{A^2}}$$ (7)

$$R_0 = R + S_{C2}$$

If the geometry is modified with a new roll radius and pipe wall thickness, the analytical solution in Table 2 and the Monte Carlo numerical method are compatible again. In this case for a point M we have: $R_0 = 0.5 + 0.0271 = 0.5271$ m, $\varepsilon^*_0 = 8.014$ E-6 m according to Table 2, while $\varepsilon^*_0 = 8.013$ E-6 according to the Monte-Carlo method.

In Figure 4 the lubricant dynamic visscosity is changed when a stronger difference of lubricant layer at increased dynamic values of a lubricant in the function ε_a is found. The results are obtained applying the Monte-Carlo numerical method. In Figure 5 the influence of ε_a on ε_0 is shown.

In Figure 6 the Contour Graphics according to the differential equation (1) and in Figure 7 the change of stress gradient in the lubricant layer according to the differential equation (2) in front of the entering section of the deformation zone L_S, Figure 1 are shown.
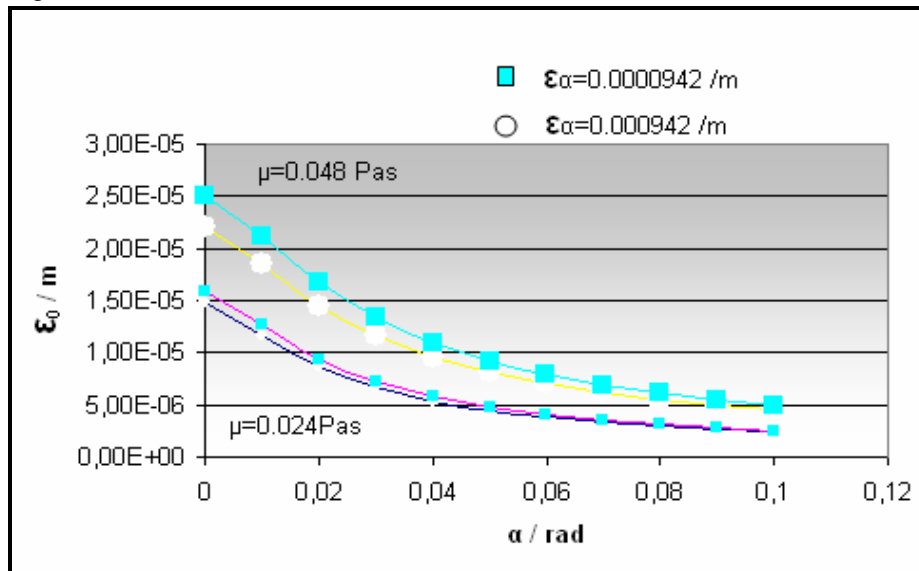

Figure 4: Influence of dynamic viscosity of lubricant and of the angle of engagement on the lubricant height at the enter section of the wall reduction zone. Monte-Carlo method.

Series 1- µ =0,024 Pas

Series 2- µ =0,048 Pas

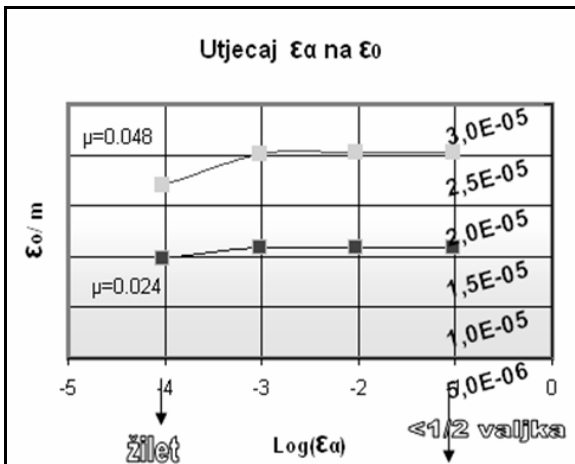Figure 5: Influence of ε_a on ε_0. It can be seen that when ε_a decreases below 1 mm, ε_a starts to influence ε_0. Monte-Carlo solution.
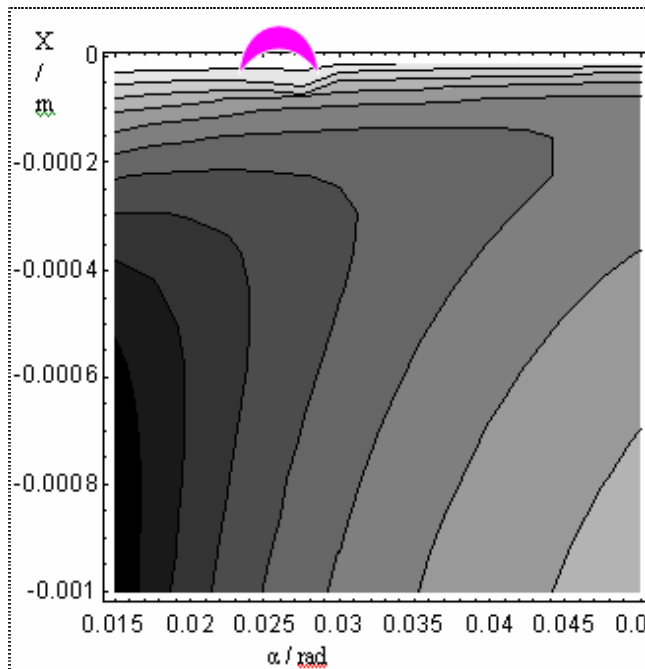

Figure 6: Contour graphics of tangential stress in the lubricant film along the x-axis in the L_R and L_S zones in the Figure 1 according to differential equation (1), Monte-Carlo solution.
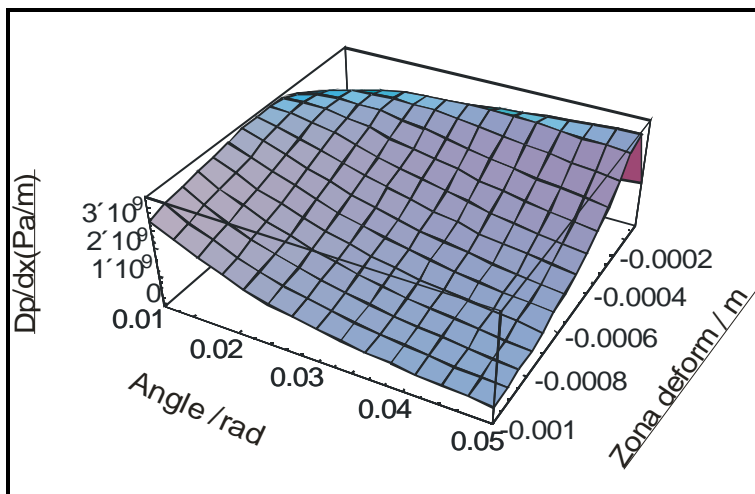
Figure 7: Diagram of the stress gradient for x=0, dp/dx is zero (approximately) and the formula Nadaia for fluid fraction in the rolling process is used.
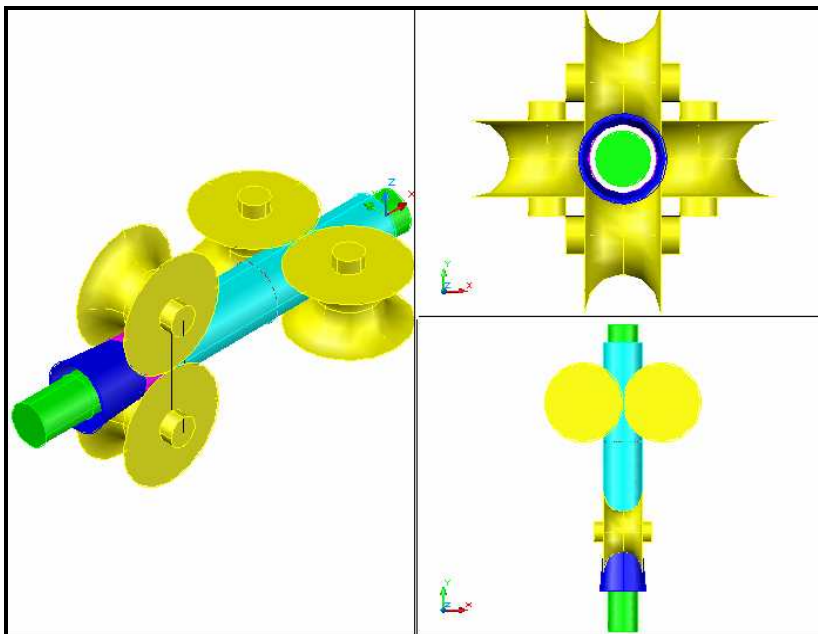

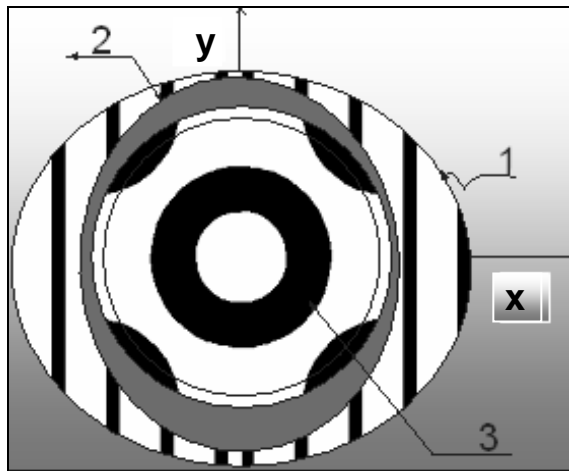Figure 8: Two rolls high mandrel rolling process of seamless pipes.

Figure 9: Ovally (ellipsoidaly) shaped lubricant layer on a mandrel due to the shape of the caliber (Figure 10, R_1 and R_2 nozzle radii of the caliber), and result of the 90 degrees caliber rotation in the mill (Figure 8), as well the result of the pipe oval shape in the final mill stands 1 and 2 – Presupposed lubricant oval shape on the mandrel 3 after passing through the first and second duo-rolls of the mill in Figure 8.

Figure 7 shows the stress gradient in the lubricant film in the zone L_S (Figure 1) in dependence on the parameters: x-axis and wall reduction angle α_0. Reological properties of lubricants and the geometry of the technological process are taken from Table 1. With the α_0 angle increase, the maximum gradient is moved towards the entering section of the deformation zone. A very similar behavior is found for tangential stresses in the lubricant layer in Figure 6. The irregularities of the graph when the engagement angle is aspiring to about 0.025 rad and the x-axis is aspiring to zero are the result of the polynomial approximation (6) where the solutions are aspiring into the complex area. This inconvenient circumstance applies also for the mathematical apparatus in the Monte-Carlo method. Therefore the approximate analytical solutions from Table 2 become even more relevant.

In Figure 8 the mechanism of the technological process where each new pair of rolls is rotated by 90 ^{0} inside the mill is shown. This technology tends to decrease the oval shape of pipes and, consequently, to decrease the oval shape of the lubricant on the mandrel, as shown in Figure 9. Since the rolls for pipe calibration are of precise dimensions and of different types, we are left with the possibility of forming lubrication pockets in the following pair of rolls where lubricant is applied over a mandrel in greater quantity (this is good from the prospective of lubrication, but it not suitable for the properties of rolled pipes). The contact effect between calibers and external pipe wall is reflected also on the contact between a mandrel and the internal pipe wall separated with the lubricant layer. The precision of rolled pipes is increased in circular calibers, but the pulling out of a mandrel is more difficult in

comparison with oval shaped calibers. The forming of lubrication pockets is more intensive with oval shaped calibers due to the nozzle radii of calibers R_1 and R_2, Figure 10. Although this effect is not of broad significance, it indicates a characteristics of the technological process which should be taken into consideration inthe accurate mathematical estimation.
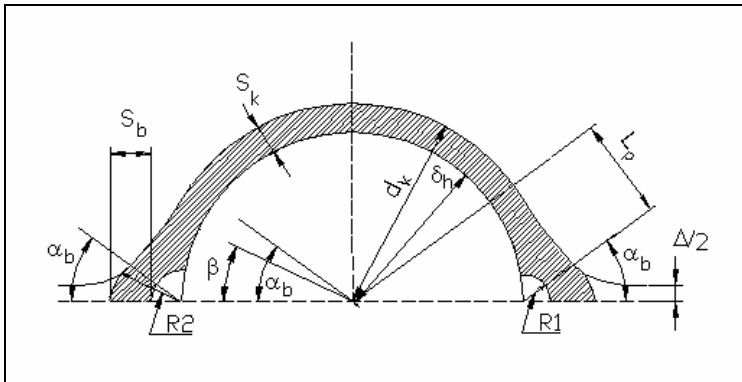

Figure 10: Calibers used in pipe rolling: 1- circular with straight nozzles, 2-circular with round nozzles, 3-oval

Practical tests show that the geometry of the mandrel also affects significantly the contact friction, even more than the already mentioned geometry of nozzles on calibers. In this area advanced research is being conducted.

3. Conclusion

The basic aim of this paper was finding approximate analytical solutions for the lubricant film in the constant rolling of seamless pipes in mills, that can not be found in references. The emphasis is given to problems of access of lubrication on the mandrel.Tthere is a possibility of lubricant milling that may, according to theoretical estimates, transform the stable hydrodynamic lubrication on the initial pairs of rolls into boundary lubrication (fraction on the insufficiently wet surfaces) on the final pairs of rolls of a mill stand.

The deduced analytical solutions (7) in the zone Ω and the point M of the zone Φ in Figure 3 are suitable for controlling the numerical method Monte-Carlo and the coordination of the results when a solution in the complex area (first of all, the coordination of an initial zero approximation) is obtained. When it is not possible to add lubricants on the last exiting mill roll pairs, the solutions can be found in reological lubricant properties (dynamic viscosity increase) or new constructions with the gradient mandrel that will change the kinematics of pipe passing in the mill. Possible solutions can be found with mandrel controlled roughness or by using oval shaped nozzles of calibers which serve as pockets for additional lubrication. One of

the possible solutions can also be the high pressure lubrication oof the surface of the mandrel.

List of symbols in equations and explanations of Figures

τ_x	Tangential stress in the lubricant film
μ	Dynamic viscosity of lubricants
μ_o	Dynamic viscosity at atmospheric pressure
γ	Piezo coefficient of lubricant viscosity
v_T	Rate of mandrel movement
v_C	Rate of tube movement
v_R	Rate of side roll
$Q(x)$	Lubricant consumption per perimeter of a pipe: $Q=0.5\,\varepsilon_o(v_T+v_R)$
$\varepsilon(x)$	Height of lubricant film in front of the deformation zone
ε_a	Lubricant height on the mandrel in front of the deformation zone(m)
ε_o	Lubricant height at the entering section of the pipe deformation zone
$\varepsilon_o^{0.1}$	Lubricant height for the engagement angle $\alpha_0=0.1$ rad
ε_o^{1}	Lubricant height when the engagement angle is 0
ε_o^{*}	Lubricant height for D=0
ε_{SR}	Approximate lubricant height after passing through rolls
ε_{aMAX}	Lubricant height which determines the M point, Figure 3, Table 2
A	Technological parameter, Table 1
D	Discriminant of the accompanying square polynom (6)
d_k	$d_k=\delta_h+2S_k$, caliber height, Figure 10
$\partial p/\partial x$ (dp/dx)	(Partial) pressure gradient in the lubricant film
α_0	Angle of pipe wall deformation
α^*	Engagement angle when D=0
α_b	Angle of caliber nozzle, Figure 10
α	Reduction angle of pipe diameter
$\alpha_b-\beta$	Constructive angle of a nozzle, Figure 10
ρ	Nozzle diameter, Figure 10
x,y	Coordinates of Decartes system
U	Rate of lubricant movement along x axis
R_0	$R_0=R+S_{C2}$
R	Roll radius
R_k	Caliber diameter, Figure 10
R_1 and R_2 – straight nozzle	Figure 10. $R_1=\rho-(\rho-R_k)\sin\alpha_b/(\sin\beta)$; $R_2=R_1-S_b$
S_{C2}	Thickness of pipe wall for the angle α_0, Table1
S_{C1}	Thickness of pipe wall after passing through rolls

S_C	Thickness of pipe wall before the rolling process
S_b	Thickness of a wall in the nozzle considering the attenuation, Figure 10
L_D	$L_D = L_R + L_S$
L_R	Projection of the reduction zone per diameter onto x axis
L_S	Projection of the deformation zone on a pipe per wall onto x axis
L_p	Length of linear part of a nozzle, Figure 10
D_C	External diameter of a pipe, Figure 2
p_0	Rolling pressure
$d_T/2$	Mandrel radius, Figure 1
Ψ	Area of the Figure 3 or the case $\varepsilon_a \gg \varepsilon_o$
Ω	Area of solutions in the Table 2 when $\alpha_0 \to 0$
Φ , Σ	Area of solutions in the Table 2 when $\varepsilon_a \to \varepsilon_0$, »lubricant milling« [Note: this ε_o^1 must be differed from ε_o^1 in the zone Ψ which is relevant in case $\varepsilon_a \gg \varepsilon_o$. Since $\varepsilon_a \to \varepsilon_0$ theoretically we reach the tripartite point: $\varepsilon_a \to \varepsilon_o^1 \to \varepsilon_0$]
M	A control point for the numerical method Monte-Carlo. It is also an indicator of the zones Φ and Σ . Figure 3 and Table 2
Razor and <1/2 of a roll	Figure 5. ε_a is scenically compared for these two cases
$Log(\varepsilon_a)$	Briggs' logarithm
Exp	Base of natural logarithm ($e \approx 2.718 \dots$)
$\Delta\varepsilon_0$	Differentiation of specific lubricant film heights on the Figure 3. Taken that the point M is realistically set in the graph maximum.
$\Delta/2$	Caliber gap, Figure 10
E-6 , $\to$, * ,[1-13], >>	10^{-6}, aspiring, multiplication sign in formulas (1) and (7), references [1-13], much larger than.
	In the Figure 6 this sign indicates conjugate complex solutions per ε_0, so we need to increase the development of a polynom in the expression (6) in applying Monte-Carlo method.[$x \to 0$;$\alpha_0 \to 0.025$ rad]. Working example according to the Table 1
$K = K(\varepsilon_0)$	Conjugate complex solutions per ε_0 (Table 3)
V and C	Roll and pipe [Figure 2]
$\varepsilon_0 = \varepsilon_0(\varepsilon_A)$	Influence of lubricant height on a mandrel on the lubricant height on the entering section of the metal deformation zone, Figure 5 Graphic display on the Figure 1 - on the left

References
1. I.Mamuzić, V.M.Drujan, Teorija, Materijali, Tehnologija čeličnih cijevi, Hrvatsko metalurško društvo, Zagreb **1996**, 137-275
2. S.V.Mazur, Postanovka zadači i zakonomernosti tečenija smazki v očage deformacii pri prokatke trub, Sučasni problemi metalurgii, **8**, 447-452 Nacionalna Metallurgičeskaja Akademia Ukraine,Dnepropetrovsk **2005**, Ukrajina
3. D.Ćurčija, I.Mamuzić, Materiali in Tehnologije, 39 (**2005**) 3, 61-77
4. O.P. Maksimenko, A.A. Semenča, Issledovanie kontaktno-gidrodinamičeskoj smazki pri prokatke. Sučasni problemi metalurgii, **8**, s. 99-103 Nacionalna Metallurgičeskaja Akademia Ukraine, Dnepropetrovsk **2005**
5. P.L. Klimenko, Kontaktniie naprjaženija pri prokatke s tehnologičeskoj smazkoj, Sučasni problemi metalurgii, **8**, 44-49 , Nacionalna Metallurgičeskaja Akademia Ukraine, Dnepropetrovsk **2005**
6. D.Ćurčija, *Materiali in tehnologije*, 37 (**2003**) 5, 237-251
7. D. Ćurčija, I. Mamuzić, *Metalurgija* 44 (**2005**) 3, 221-226
8. D. Ćurčija, I. Mamuzić, *Metalurgija* 44 (**2005**) 4, 295-300
9. D. Ćurčija, I. Mamuzić, Oblik mazivog sloja kod dresiranja trake , 38. simpozij Maziva 2005, Rovinj 19.-21.10. **2005**.
10. D.Ćurčija, I.Mamuzić, *Metalurgija* 43 (**2004**) 249
11. D.Ćurčija, I.Mamuzić, *Goriva i Maziva* 46 (**2007**) 1, 34-44.
12. D.Ćurčija, I.Mamuzić , F.Vodopivec, *Metalurgija* 45 (**2006**) 3, 250.
13. D.Ćurčija, I.Mamuzić, *Materiali in tehnologije*, 41 (**2007**)1, 21-27.

Authors
Dušan Ćurčija, M.Sc.; e-mail: plutonijanac21@net.hr
prof.dr.sc. Ilija Mamuzić, M.Sc..; Metallurgical faculty Sisak, University of Zagreb